Binding Pathway of Retinal to Bacterio-Opsin: A Prediction by Molecular Dynamics Simulations

Barry Isralewitz,*# Sergei Izrailev,*§ and Klaus Schulten*#§
*Beckman Institute for Advanced Science and Technology; #Center for Biophysics and Computational Biology; and §Department of Physics, University of Illinois, Urbana, Illinois 61801 USA

ABSTRACT Formation of bacteriorhodopsin (bR) from apoprotein and retinal has been studied experimentally, but the actual pathway, including the point of entry, is little understood. Molecular dynamics simulations provide a surprisingly clear prediction. A window between bR helices E and F in the transmembrane part of the protein can be identified as an entry point for retinal. Steered molecular dynamics, performed by applying a series of external forces in the range of 200–1000 pN over a period of 0.2 ns to retinal, allows one to extract this chromophore from bR once the Schiff base bond to Lys^{216} is cleaved. Extraction proceeds until the retinal tail forms a hydrogen bond network with Ala^{144}, Met^{145}, and Ser^{183} side groups lining the exit/entry window. The manipulation induces a distortion with a fitted root mean square deviation of coordinates (ignoring retinal, water, and hydrogen atoms) of less than 1.9 Å by the time the retinal carbonyl reaches the protein surface. The forces needed to extract retinal are due to friction and do not indicate significant potential barriers. The simulations therefore suggest a pathway for the binding of retinal. Water molecules are found to play a crucial role in the binding process.

INTRODUCTION

Bacteriorhodopsin (bR) (Khorana, 1988; Birge, 1990; Oesterhelt et al., 1992; Lanyi, 1992; Krebs and Khorana, 1993; Khorana, 1993; Schulten et al., 1995) is a light-driven vectorial proton pump found in the membrane of *Halobacterium salinarum*. The seven-helix protein contains a retinal molecule joined through a Schiff base linkage to its Lys^{216} side group (Bayley et al., 1981). Formation of bR from the folded apoprotein bacterio-opsin (bO) and retinal has been observed experimentally (Oesterhelt et al., 1973; Oesterhelt and Schumann, 1974; Oesterhelt et al., 1974; Huang et al., 1981; Towner et al., 1981; Chang et al., 1988; Booth et al., 1996). The binding reaction involves an intermediate, I_2, obeying second-order kinetics (Booth et al., 1996). The location of retinal within bR after binding, and the binding for various analogs of retinal have been well studied (Zingoni et al., 1986; Crouch, 1986; Gat and Sheves, 1993; Humphrey et al., 1994; de Lera et al., 1995), but the path followed by retinal during bR formation is unknown.

Retinal exhibits much greater affinity for a lipid environment than for water (McCaslin and Tanford, 1981; London and Khorana, 1982; Ho et al., 1989; Szuts and Harosi, 1991). Therefore, it is likely that complexation of retinal with bO initiates on the hydrophobic (i.e., lipid-covered) surface rather than in the water-solvated loop regions of the protein (Renthal et al., 1995). Examination of bR's transmembrane region reveals, indeed, a suitable opening located between helices E and F of bR, through which the β-ionone ring is visible from the outside. This opening, shown in Fig. 1, appears to provide an entrance for retinal.

In the closely related protein rhodopsin, in which retinal unbinding and binding occur as part of the vision cycle, the corresponding helix F is seen to move upon retinal's 11-*cis* → all-*trans* isomerization, opening an unbinding/binding pathway (Farrens et al., 1996). Such a pathway is also suggested by electron microscopy data of frog rhodopsin (Unger et al., 1997) showing that the distance between helices 5 and 6 (which correspond to bR helices E and F) is greater than that of any other pair of neighboring helices in rhodopsin.

One can test, by means of molecular dynamics (MD) simulations, the possibility of retinal entering bR through the putative entry window between the E and F helices by extracting retinal from bR along a path from its bound position toward and out of the stated window. If the protein structure is not disrupted during such an extraction, and if the folded bR structure without retinal is similar to that of intermediate I_2 (in the sequence 1) $bO \rightarrow I_1 \rightarrow I_2 \overset{+R}{\rightarrow} I_R$, followed by the two-step Schiff base formation $I_R \rightarrow I_3 \rightarrow$ bR; Booth et al., 1996), then one could argue that the resulting unbinding path also constitutes the path of retinal's binding to bO. In this paper we examine this possibility, using so-called steered MD simulations (Grubmüller et al., 1996; Izrailev et al., 1997; Balsera et al., 1997). The method applies a series of external forces to retinal to pull the chromophore out of its binding pocket in the course of an MD simulation. The calculations have been inspired by recent experimental work in manipulating molecules, such as atomic force microscopy (Florin et al., 1994), biomembrane force probe (Evans et al., 1994, 1995), and optical tweezers (Block and Svoboda, 1994), as well as by theoretical investigations (Evans and Ritchie, 1997).

Received for publication 5 June 1997 and in final form 17 September 1997.
Address reprint requests to Dr. Klaus Schulten, Department of Physics, Beckman Institute 3147, University of Illinois, 405 N. Mathews Ave., Urbana, IL 61801. Tel.: 217-244-1604; Fax: 217-244-6078; E-mail: kschulte@ks.uiuc.edu.

0006-3495/97/12/2972/08 $2.00

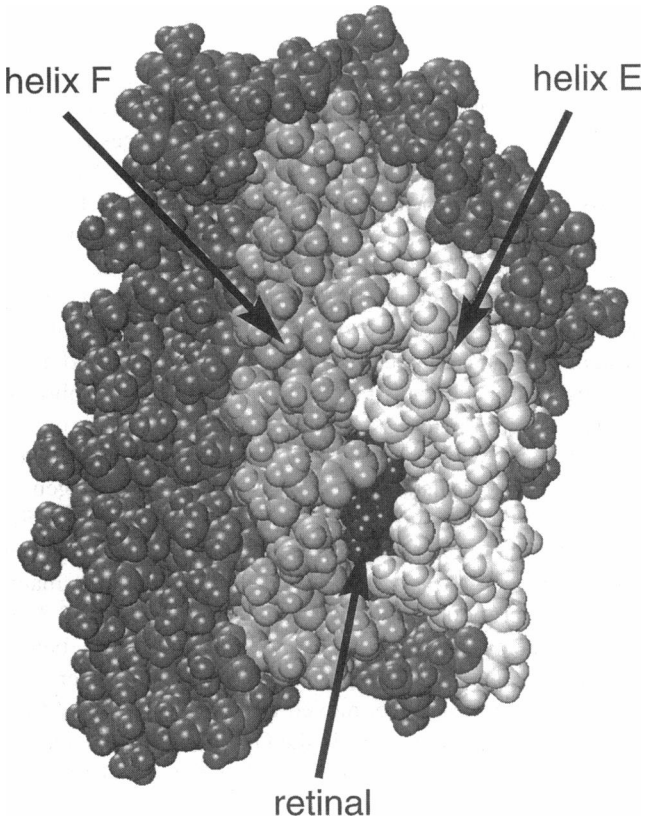

FIGURE 1 Initial structure of bacterio-opsin with retinal bound, presented with van der Waals spheres. Retinal can be seen between helices E and F through the only opening of this size in the membrane-exposed surface of the protein.

METHOD

MD simulations of native bR were carried out using the program X-PLOR (Brünger, 1992) with the CHARMM19 (Brooks et al., 1983) force field. The structure of bR taken as the initial model was based on crystallographic data (Henderson et al., 1990), which was further refined (Nonella et al., 1991; Humphrey et al., 1994). In the transmembrane region, this structure is similar (RMS deviation of 2.1 Å) to a more recent experimental bR structure (Grigorieff et al., 1996). Sixteen water molecules were present in the interior of the protein, as placed by Humphrey et al. (1994). The modeled bR was modified through cleavage of the retinal Schiff base, resulting in a Lys^{216} side group with an immediately adjacent retinal. The part of the structure within 4 Å of the retinal carbonyl group was then energy minimized. The resulting structure represents the apoprotein bacterio-opsin (bO) complexed with retinal, without Schiff base linkage. This structure involves a very strong hydrogen bond connecting the retinal carbonyl and Lys^{216} nitrogen, whereas in bR retinal is covalently bonded to the lysine. Charge distribution and force constants for retinal as reported by Humphrey et al. (1994) were used. An overview of MD simulations on bR is provided by Schulten et al. (1995).

The system was simulated in vacuum. In the simulations we assumed a dielectric constant $\epsilon = 1$ and cutoff Coulomb forces with a switching function starting at a distance of 10 Å and reaching zero at 12 Å. A time step of integration of 1 fs was employed. All atoms, including hydrogens, were treated explicitly. The modified bR structure underwent 20 ps of equilibration in a thermal bath at $T = 300$ K, followed by 5 ps of free dynamics.

Preliminary runs (data not shown) indicated that the forced unbinding of retinal destroys the structure of the protein, unless water molecules are in the immediate vicinity of the retinal-Lys^{216} contact. Therefore, as the starting point of steered MD simulations, we chose from a trajectory of the bO-retinal complex a structure in which two water molecules had moved close to this contact.

The extraction of retinal from bR was performed by application of external forces to retinal. These forces were implemented by restraining the center of retinal's β-ionone ring harmonically to a restraint point and moving the restraint point with a constant velocity v in a desired direction. The procedure is equivalent to attaching one end of a harmonic spring to the β-ionone ring of retinal and pulling on the other end. The exerted force is then

$$F = kd \tag{1}$$

where k is the force constant, and d is the distance between the center of retinal's β-ionone ring and the restraint point. We chose k to be 10 $k_BT/Å^2$ and v to be 0.125 Å/ps. These values of the force constant and the velocity correspond to a stiff spring in the drift regime (Evans and Ritchie, 1997; Izrailev et al., 1997) and allow spatial fluctuations of the center of the retinal ring of magnitude $\delta x = \sqrt{k_BT/k} = 0.32$ Å. To realize a movement of the restraint point with nearly constant velocity, the position of the restraint point was changed every 100 fs by a distance of $v \times (100$ fs) in the desired direction. The alpha carbons of six residues, at the ends of helices A, B, and C of bR, were held fixed to prevent lateral movement of bO.

Due to the convoluted shape of the retinal binding site, retinal cannot be extracted from bR by application of a force along a straight line (data not shown). Therefore, we segmented the unbinding path, determining a direction of the restraint point movement anew for each segment. In our simulations we constructed an unbinding path consisting of 10 such segments. For this purpose we employed a trial and error approach, in which for each segment retinal was pulled in a chosen direction for 20 ps, during which the changes in the protein, such as changes in temperature, secondary structure, positions of water molecules, progress of retinal towards the exit, etc., were monitored. For each segment we chose three likely directions of the path and tested them, starting with a zero applied force. The trial directions were chosen according to their anticipated impact on the different characteristics of the protein. For example, one direction might be considered better for preventing a helix from distorting, whereas another might be considered more likely to loosen the bond between retinal and Lys^{216}. The actual success of the tested directions was then evaluated on

TABLE 1 Considerations for choosing trial directions and evaluating resulting paths

Property	Choice of trial directions	Evaluation of resulting paths
Secondary structure (SS)	Avoid regions where SS has been distorted	Choose paths preserving SS
van der Waals (VDW) interactions	Avoid collisions of ligand with the protein	Find paths with minimal interaction, allowing further movement
Bond rupture progress	Parallel to the bond	Choose paths with larger distance between atoms forming the bond
Positions/orientations of water molecules	No effect	To rupture an H-bond, choose paths with waters closest to the H-bond and oriented to disrupt the bond
Local RMSD	Avoid regions where RMSD has been increasing	Choose paths maintaining RMSD close to 1 Å
Local temperature (T)	Avoid regions where T has been increasing	Choose paths maintaining T

the basis of the changes in the protein. The trajectory corresponding to the best direction was selected to provide the initial structure for the next segment. The selection process was then repeated, starting with the choice of three new directions based on this new initial structure. In cases where none of the trajectories were acceptable, a new set of directions was tested. Some of the monitored characteristics of the system and their influence on the decision to accept a given direction are summarized in Table 1.

The analysis of possible trial directions was performed entirely with the aid of the molecular visualization program VMD (Humphrey et al., 1995; Dalke and Schulten, 1997), which allows one to represent and analyze various aspects of molecular structures in an intuitive manner, using VMD's built-in scripting language. The secondary structure of the protein was determined by the program STRIDE (Frishman and Argos, 1995) and then displayed and analyzed with VMD. Fig. 2 illustrates retinal and its binding pocket in bR for one of the segments mentioned above.

RESULTS

To determine a possible unbinding path of retinal, the chromophore was pulled along a segmented path out of its binding site by means of external forces as described in Methods. The simulations revealed several distinct features of the unbinding process. Four stages of the process are presented in Fig. 3. The first segment of the path served to reorient retinal, to allow its exit along the narrow path leading to the opening between helices E and F. A proper orientation of retinal was achieved during a 9.2-ps simulation, with the restraint point moving at a velocity of 1 Å/ps. The resulting structure had retinal aligned along a straight line from the retinal-Lys^{216} hydrogen bond toward the opening (shown in Fig. 3 *b*). During the following three segments of the unbinding path, the main obstacle to retinal's exit from the binding site was the hydrogen bond between retinal's carbonyl group and Lys^{216} of bR. This bond remained intact during the simulation, until a water molecule located in the vicinity of the bond formed a bridge between

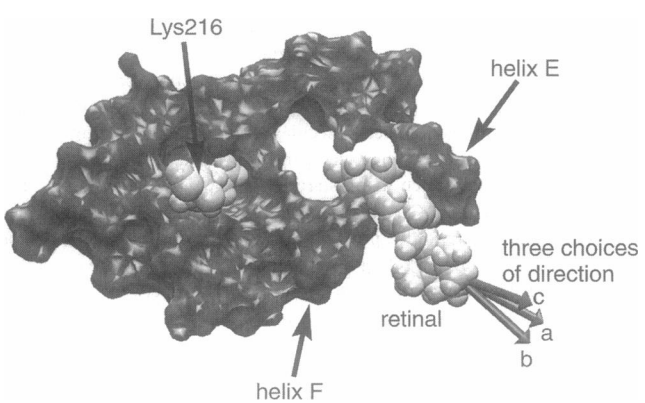

FIGURE 2 Retinal, Lys^{216}, and the molecular surface of a 5-Å slice of bacterio-opsin at t = 69.2 ps, the end of the 4th pulling segment. The view is down the axis of the helices, with a slice of helix E and F on both sides of retinal. This representation facilitated the choice of trial directions for the following pulling segment. The arrows indicate the chosen trial directions for the forces that were applied during the three simulations of the following segment. Pulling direction a avoids moving the retinal toward helix F, whereas pulling direction b avoids helix E. Pulling direction c avoids helix F, and is aimed out of the page to keep retinal away from residues below it, which is not visible in this representation.

lysine and retinal, allowing the bond to break at t = 62.3 ps (see Figs. 3 *c* and 4). After the water bridge was broken during the third segment at t = 68.6 ps, retinal moved within 12 ps through the opening until it was completely outside bR. At that time retinal had passed helices E and F; its carbonyl oxygen formed a stable network of hydrogen bonds with Ala^{144}, Met^{145}, and Ser^{183} on these helices, as shown in Figs. 3 *d* and 5. The last 110 ps of the simulation were aimed at testing the strength of this network.

The simulated unbinding path allows retinal's exit from bO without significantly disturbing the structure of the protein. The data characterizing the process of unbinding in this regard are shown in Figs. 6 and 7. The force applied to retinal along its path is presented in Fig. 6 *a*. The progress in the retinal-Lys^{216} hydrogen bond rupture was monitored through the O-N distance between the carbonyl oxygen of retinal and the ϵ-amino nitrogen of Lys^{216}, presented in Fig. 6 *b*. The bond remained stable until the formation of a water bridge between retinal and Lys^{216}. This process was manifested by a pronounced jump in the O-N distance at 62.3 ps, which plateaued between 4 Å and 5 Å for 5 ps before increasing again, when retinal, together with the water molecule forming the bridge, moved away from Lys^{216}. At the moment of the first increase in the O-N distance, the applied force reached a local maximum of 970 pN and then dropped to ~500 pN, due to retinal's movement toward the restraint point, decreasing d as defined in Eq. 1. At the second jump of the O-N distance, the applied force dropped from 500 to ~300 pN, and stabilized at this level. The force remained small because there were no hydrogen bond donors along the path that could bond with the retinal carbonyl oxygen. Such bonds, if formed, would prevent further motion of retinal in the pulling direction, thus causing the applied force to increase.

During the retinal-Lys^{216} hydrogen bond rupture, the potential energy stored in the restraint and in the deformation of the protein was released (see Fig. 6 *c*), resulting in a temperature increase of 40 K.

The changes in the protein structure were monitored through the root mean square deviation (RMSD) of the heavy atom coordinates from those of the initial structure, as well as through the changes in the secondary structure (see Fig. 7). The RMSD did not exceed 1.8 Å until after retinal had exited bO and formed the hydrogen bond network with Ala^{144}, Met^{145}, and Ser^{183} of helices E and F. The percentage of residues forming the same secondary structure as the initial structure (helix identity) remained over 90% until the hydrogen bond network formed.

During the last 110 ps of the trajectory, the hydrogen bond network between retinal and helices E and F remained stable despite the applied force, even though the latter increased from 300 pN to ~400 pN during the final 50 ps of the simulation. During this time the applied force also caused a significant protein deformation, manifested by an increase in the RMSD and a decrease in the percentage of residues forming α-helices. The stability of the hydrogen bond network can be explained by the absence of a water-

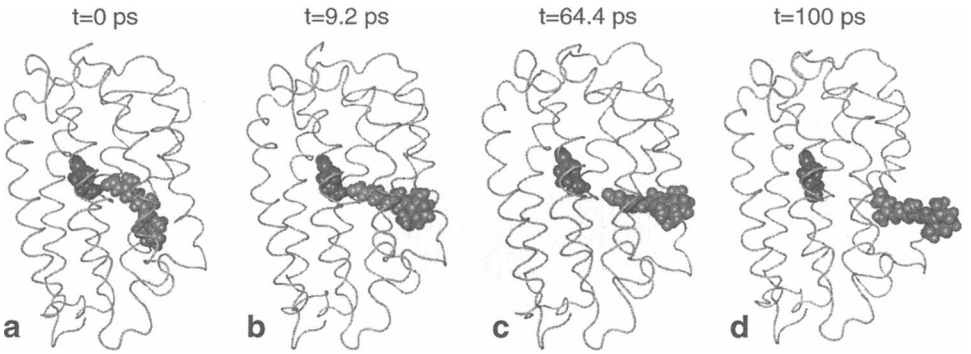

FIGURE 3 Bacterio-opsin and retinal at four stages of the simulation. The protein backbone is shown in tube representation; Lys^{216} and retinal are presented as van der Waals spheres. (*a*) $t = 0$ ps; (*b*) $t = 9.2$ ps; (*c*) $t = 64.4$ ps (see also Fig. 4); (*d*) $t = 100$ ps (see also Fig. 5).

lipid environment around the protein in the simulations, because the energy cost of breaking the hydrogen bond network would not be compensated by interactions of retinal and helix E, F side chains with water or lipid molecules.

The changes of the structure of bO determined our strategy for choosing and evaluating the trial directions of the segmented unbinding path. Initially, the choice focused on moving retinal's β-ionone ring close to the exit window. Later, the focus shifted to breaking the hydrogen bond between retinal and Lys^{216}. After the retinal-lysine bond was broken, the main focus was the preservation of the protein helices, especially helices E and F. The final focus was on a test of the strength of the hydrogen bond network between retinal's carbonyl oxygen and Ala^{144}, Met^{145}, and Ser^{183}.

We performed control experiments to test other possibilities of retinal's exit from bR. For this purpose, we carried out a series of simulations employing a high-velocity (1 Å/ps) displacement of the restraint point and a number of straight-line paths, directed between helices E and F as well as between other helix pairs, and through the cytoplasmic and periplasmic faces of bO. The resulting distortions of the protein structure were much larger than for the path described above. However, no strict conclusions can be drawn from these trials, because of the short time scales (10–35 ps) involved.

DISCUSSION

Steered MD provides details of unbinding processes induced by the application of external forces. These forces are not constrained by limitations arising in experiment, thus allowing great flexibility in the direction, magnitude, and position where the forces are applied. In this work we have extended the steered MD technique (Grubmüller et al., 1996; Izrailev et al., 1997) to a segmented, interactive manipulation of a ligand, allowing alterations to the applied forces to thread a ligand out of a binding pocket.

Transition from bacteriorhodopsin formation stage I_2 to stage I_R in the $bO \rightarrow I_1 \rightarrow I_2 \overset{+R}{\rightarrow} I_R \rightarrow I_3 \rightarrow bR$ sequence takes place on a time scale of seconds (Booth et al., 1996); the extraction of retinal in our simulations is completed in ~100 ps, a time 10 orders of magnitude shorter. Such a time scale gap and the fact that the unbinding is a nonequilibrium

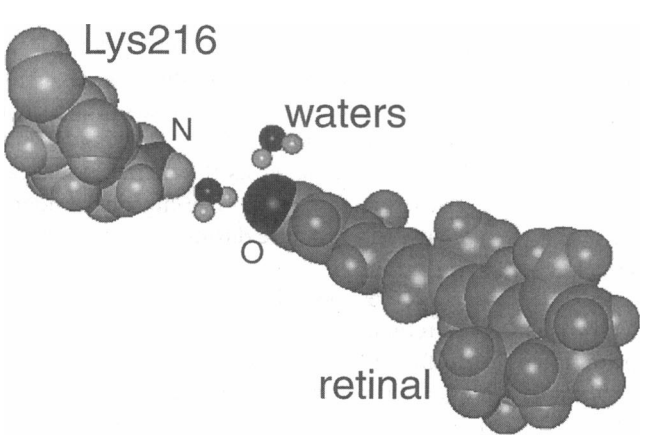

FIGURE 4 The water bridge between retinal's carbonyl oxygen and the amino nitrogen of Lys^{216} at $t = 64.4$ ps (see also Fig. 3 *c*). Two of the 16 waters in the structure are shown. One water is hydrogen-bonded to retinal, and the other is hydrogen-bonded to both retinal and lysine, forming a bridge.

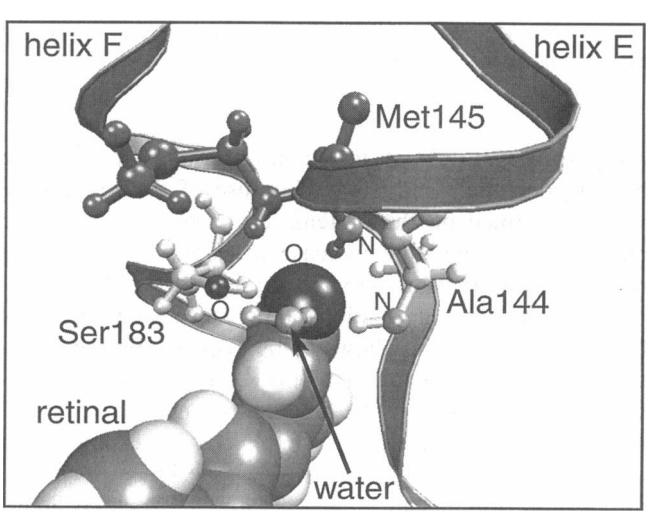

FIGURE 5 The hydrogen bond network formed by retinal's carbonyl with the amide nitrogen of Ala^{144}, the amide nitrogen of Met^{145}, and the γ-oxygen of Ser^{183} as retinal exits bacterio-opsin at $t = 100$ ps (see also Fig. 3 *d*).

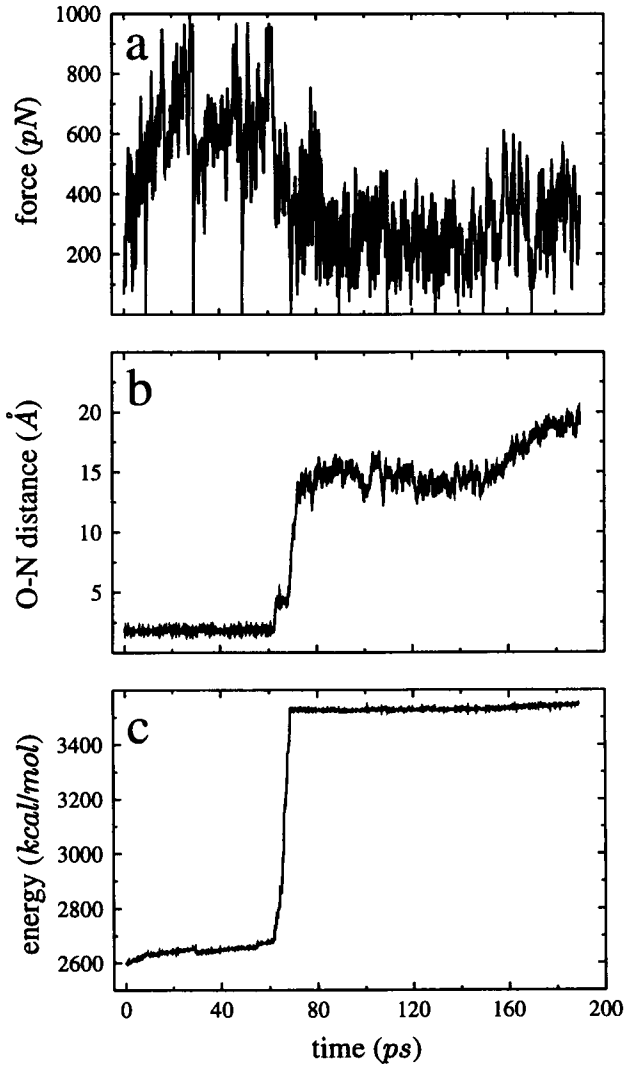

FIGURE 6 Characteristics describing the progress of retinal toward the exit window during the simulation. (*a*) Force exerted on the retinal head group by the restraint. (*b*) Distance between the retinal carbonyl oxygen and the ϵ-nitrogen of Lys^{216}. (*c*) Total potential energy of the system, excluding the energy of restraint.

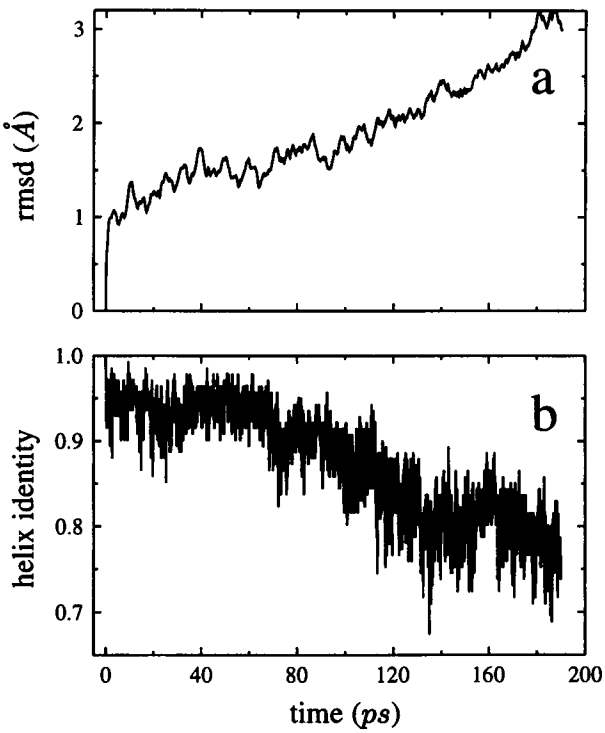

FIGURE 7 Characteristics describing the stability of bacterio-opsin structure during the simulation. (*a*) RMS deviation from the initial structure, ignoring hydrogens, water, and retinal. (*b*) Helix identity of residues in helices A–G. Helix identity measures the percentage of residues that form the same secondary structure as the initial structure; helix identity has been determined for all residues defined as members of helices A–G by Henderson et al. (1990).

process make it difficult to obtain quantitative data on the binding potentials and forces, because of the irreversible work performed on the system. This work results in the energy and temperature increase observed. However, the unbinding observed in the simulations performed still provides qualitative information about steric and hydrogen bond interactions, and allows comparison of binding properties of related molecular systems (Izrailev et al., 1997) as well as evaluation of the binding potential (Evans and Ritchie, 1997; Balsera et al., 1997). The forces applied in our steered MD simulations have been designed to enforce a transition from a state I_R just before the events of Schiff base formation to a state I_2 immediately preceding retinal entry. The simulations assumed that there are no significant changes in protein structure during the transition from I_R to bR. This assumption will hold true if the structural changes observed between bO and bR (Acuña et al., 1984; Cladera et al., 1996), from a relatively open configuration of the helices to a more compact one, take place after the formation of I_2 and before the formation of I_R in the bR formation sequence.

Preservation of helix identity is an important test of the validity of our simulations, since experimental evidence has shown high conservation of helical structure when bR is bleached to bO, an even earlier intermediate than I_2 (Cladera et al., 1996). This testing criterion is also supported by the two-stage model of membrane protein folding (Popot and Engelman, 1990), which suggests that helix formation precedes tertiary structure formation. The high helix identity observed in the protein structure during the extraction of retinal satisfies this criterion.

The magnitude of the applied force was not the only determinant of the retinal-Lys^{216} hydrogen bond rupture in the simulations. In fact, the force applied to retinal reached peak values (of over 900 pN) not only at the time of rupture (at t = 62.3 ps), but also before rupture. Residues and water molecules in the binding pocket also contributed significantly to the total force experienced by retinal and, therefore, affected the bond rupture. At the moment of the retinal-Lys^{216} bond rupture, two water molecules formed hydrogen bonds with the retinal carbonyl oxygen. To allow

formation of such bonds, we started the simulation at an instance in a free dynamics trajectory of bR when two of the 16 water molecules included in the simulation (see Method) had come close to the retinal-lysine hydrogen bond, thus weakening the bond. In simulations without water positioned this way, the retinal-lysine bond ruptured only after the applied forces had greatly distorted the protein (RMSD values over 10 Å).

Once the lysine-retinal hydrogen bond had been broken, the retinal carbonyl passed through the exit window within 12 ps. During this time period the applied force dropped to 300 pN. The fast movement and small force imply an unobstructed path for retinal unbinding. The path chosen is thus likely to furnish a viable path for retinal binding.

At the exit window, the retinal carbonyl formed a hydrogen bond network to residues Ala^{144}, Met^{145}, and Ser^{183}. This suggests that these residues attract the retinal carbonyl and steer the chromophore into the binding pocket. Water may play an important role in liberating retinal from these residues and in building a bridge to Lys^{216}. In fact, water molecules are required for the Schiff base to form (Rousso et al., 1995).

Many of the residues lining the exit window are conserved in type in proteins homologous to bR. The only residues in the vicinity of the entry window that are perfectly conserved between bR and the 15 top scoring BLAST (Altschul et al., 1990) aligned sequences (with a smallest sum probability less than 10^{-13}) were Trp^{182}, Tyr^{185}, and Pro^{186}. The residues we observed participating in the hydrogen bond network at helices E and F, Ala^{144}, Met^{145}, and Ser^{183}, are not conserved. However, because two of the three residues, Ala^{144} and Met^{145}, bind retinal carbonyl with backbone amide groups, a general similarity in the entry area of residue size and hydrogen bond donor pattern should be sufficient to allow retinal entry.

We have compared our simulation results to observations that examine reconstitution rates in bR mutants (Hackett et al., 1987; Mogi et al., 1987, 1988, 1989a,b; Filtsch and Khorana, 1989; Stern and Khorana, 1989; Greenhalgh et al., 1991; Marti et al., 1991a,b; Mierke et al., 1991; Subramaniam et al., 1991; Greenhalgh et al., 1993; Altenbach et al., 1994) and in chemically altered bR (Greenhalgh et al., 1993; Altenbach et al., 1994; Renthal et al., 1995). Some experimental modifications with significant effects on bR reconstitution lie along the putative unbinding pathway, whereas others do not. The effects of these modifications on all-*trans*-retinal reconstitution rates are summarized in Table 2. Thirteen modifications along the binding path have been observed to have little effect on the reconstitution rate. (A modification was considered to cause an increase (decrease) in the regeneration rate if it caused a 30% decrease (100% increase) in the $t_{1/2}$ for chromophore regeneration. A residue was considered to be along the binding pathway if it lay within 3 Å of Lys^{216} or within 5 Å of retinal as the latter moved along the pathway.) However, of the 10 modifications observed to significantly increase the reconstitution rate, nine are along the binding pathway. The tenth, P50G, allows freer backbone movement, and thus likely affects the position of Val^{49}, an adjacent residue that is along the pathway and has been shown to affect reconstitution. All 10 rate-increasing modifications may affect binding in the same way, by creating a more open pathway for retinal movement.

Three mutations of a polar to a negatively charged residue along the pathway (T89D, M118E, and M145E) resulted in reduced reconstitution rates; such an effect is consistent with unfavorable interactions of the negatively charged residues with retinal's carbonyl group. Of all modifications that significantly reduce reconstitution rates, modifications that are not along the binding pathway outnumber modifications that are along the pathway. The former modifications may slow reconstitution by preventing backbone conformational changes required for retinal binding.

TABLE 2 Summary of bR modification experiments: effects on all-*trans*-retinal regeneration rates

Change in rate	On path	Modification
No effect	Yes	M20A/E[m], R82Q[d], W86F[g], T90C[e], L93A/V[h], I117C[n], M118A[m], T121V[j], W137F/C[g], S141A[j], T142V[j], S183A[b], W189F[b]
No effect	No	R7Q[d], W10F[g], W12F[g], T24V[j], Y26F[a], D36N[c], D38N[c], T55V[j], S59A[j], Y64F[a], G72C[e], E74C[l], N76C[l], D96E[c], D96C[l], A98C[l], V101C[l], D102N[c], A103C[l,n], Q105C[l,n], T107V[j], L109C[l,n], G113C[n], G116C[n], G120-meth[n], V124C/meth[n], L127C[n], T128V[j], K129C/meth[n], Y131F[a], S132A[j], Y150F[a], T157V[j], S158A[j], R164Q[d], S193A[b,j], E194Q[b], R225Q[d], R227Q[d]
Increase	Yes	V49A[m], D85E[c,i], L93T[h], R134Q[d], W138F[g], S141C[j], M145A[m], P186G[f], W189F[g]
Increase	No	P50G[f]
Decrease	Yes	V49L[m], A53G[m], R82Q[i,k], R82C/meth[l], Y83F[a], D85N[c,i,k], D85C/meth[l], T89V/A/D[j], T90V[j], I117-meth[n], M118E[m], Y133F[a], M145E[m], Y147F[a], W182F[b,g], S183A[j], Y185F[a,b], P186L[b], P186A/V[f], D212A[c], D212E/N[c,i], S214A[j]
Decrease	No	T17V[j], Y43F[a], T46V[j], T47V[j], P50A[f], Y57F[a], E74-(ETC modified)[o], E74-meth[l], N76-meth[l], Y79F[a], Y79C/meth[l], P91A/G[f], L92C[e], D96N[c,k], D96-meth[l], A98-meth[l], V101-meth[l], A103-meth[l,n], D104N[c], Q105-meth[l,n], L109-meth[l,n], G113-meth[n], D115N/E[c], G116-meth[n], G120C[n], G122C[m], L127-meth[n], S169C[e], R175Q[d], T178V[j], T205V[j], S226A[j]

[a] Mogi et al. (1987); [b] Hackett et al. (1987); [c] Mogi et al. (1988); [d] Stern and Khorana (1989); [e] Filtsch and Khorana (1989); [f] Mogi et al. (1989b); [g] Mogi et al. (1989a); [h] Subramaniam et al. (1991); [i] Marti et al. (1991b); [j] Marti et al. (1991a); [k] Mierke et al. (1991); [l] Greenhalgh et al. (1991); [m] Greenhalgh et al. (1993); [n] Altenbach et al. (1994); [o] Renthal et al. (1995).

Notation: meth, methanethiosulfonate derivatized cysteine; ETC, 1-ethyl-3-[3-(trimethylamino)-propyl]carbodiimide.

New mutation experiments designed to block the entry window will more convincingly establish if the proposed binding pathway of retinal is relevant for bR reconstitution. In particular, we expect that mutations increasing the size of Ala^{143}, Ala^{144}, and Ser^{183} (e.g., A143F, A144F, S183Y) decrease the reconstitution rate, and thereby may pinpoint retinal's site of entry into bR.

The authors thank A. Balaeff, A. Dalke, and S. Stepaniants for fruitful discussions.

This work was supported by grants from the National Institutes of Health (PHS 5 P41 RR05969-04), the National Science Foundation (BIR-9318159, BIR 94-23827 (EQ), DMR-93-14938), and the Roy J. Carver Charitable Trust. BI was partially supported by the Beckman Institute for Advanced Science and Technology and by a GAANN Fellowship from the U.S. Department of Education.

REFERENCES

Acuña, A. U., J. González, M. Lillo, and J. Otón. 1984. The UV protein fluorescence of purple membrane and its apomembrane. *Photochem. Photobiol.* 40:351–359.

Altenbach, C., D. A. Greenhalgh, H. G. Khorana, and W. L. Hubbell. 1994. A collision gradient method to determine the immersion depth of nitroxides in lipid bilayers: application to spin-labeled mutants of bacteriorhodopsin. *Proc. Natl. Acad. Sci. USA.* 91:1667–1671.

Altschul, S. F., W. Gish, W. Miller, E. W. Myers, and D. J. Lipman. 1990. Basic local alignment search tool. *J. Mol. Biol.* 215:403–410.

Balsera, M., S. Stepaniants, S. Izrailev, Y. Oono, and K. Schulten. 1997. Reconstructing potential energy functions from simulated force-induced unbinding processes. *Biophys. J.* 73:1281–1287.

Bayley, H., K.-S. Huang, R. Radhakrishnan, A. H. Ross, Y. Takagaki, and H. G. Khorana. 1981. Site of attachment of retinal in bacteriorhodopsin. *Proc. Natl. Acad. Sci. USA.* 78:2225–2229.

Birge, R. R. 1990. Nature of the primary photochemical event in rhodopsin and bacteriorhodopsin. *Biochim. Biophys. Acta.* 1016:293–327.

Block, S., and K. Svoboda. 1994. Biological applications of optical forces. *Annu. Rev. Biophys. Biomol. Struct.* 23:247–285.

Booth, P. J., A. Farooq, and S. L. Flitsch. 1996. Retinal binding during folding and assembly of the membrane protein bacteriorhodopsin. *Biochemistry.* 35:5902–5909.

Brooks, B. R., R. E. Bruccoleri, B. D. Olafson, D. J. States, S. Swaminathan, and M. Karplus. 1983. CHARMm: a program for macromolecular energy, minimization, and dynamics calculations. *J. Comp. Chem.* 4:187–217.

Brünger, A. T. 1992. X-PLOR, Version 3.1: A System for X-Ray Crystallography and NMR. Howard Hughes Medical Institute and Department of Molecular Biophysics and Biochemistry, Yale University, New Haven, CT.

Chang, C.-H., R. Jonas, R. Govindjee, and T. Ebrey. 1988. Regeneration of blue and purple membranes for deionized bleached membranes of *Halobacterium halobium*. *Photochem. Photobiol.* 47:261–265.

Cladera, J., J. Torres, and E. Padrós. 1996. Analysis of conformational changes in bacteriorhodopsin upon retinal removal. *Biophys. J.* 70: 2882–2887.

Crouch, R. K. 1986. Studies of rhodopsin and bacteriorhodopsin using modified retinals. *Photochem. Photobiol.* 44:803–807.

Dalke, A., and K. Schulten. 1997. Using TCL for molecular visualization and analysis. *In* Proceedings of the Pacific Symposium on Biocomputing 97 on Interactive Molecular Visualization. 85–96.

de Lera, A. R., B. Iglesias, J. Rodríguez, R. Alvarez, S. López, X. Villanueva, and E. Padrós. 1995. Experimental and theoretical analysis of the steric tolerance of the binding site of bacterioopsin with the use of side-chain methyl-shifted retinal analogs. *J. Am. Chem. Soc.* 117: 8220–8231.

Evans, E., R. Merkel, K. Ritchie, S. Tha, and A. Zilker. 1994. Picoforce method to probe submicroscopic actions in biomembrane adhesion. *In* Studying Cell Adhesion. P. Bongrand, P. M. Claesson, and A. S. G. Curtis, editors. Springer-Verlag, Berlin. 125–140.

Evans, E., and K. Ritchie. 1997. Dynamic strength of molecular adhesion bonds. *Biophys. J.* 72:1541–1555.

Evans, E., K. Ritchie, and R. Merkel. 1995. Sensitive force technique to probe molecular adhesion and structural linkages at biological interfaces. *Biophys. J.* 68:2580–2587.

Farrens, D. L., C. Altenbach, K. Yang, W. L. Hubbell, and H. G. Khorana. 1996. Requirement of rigid-body motion of transmembrane helices for light activation of rhodopsin. *Science.* 274:768–770.

Filtsch, S. L., and H. G. Khorana. 1989. Structural studies on transmembrane proteins. 1. Model study using bacteriorhodopsin mutants containing single cysteine residues. *Biochemistry.* 28:7800–7805.

Florin, E.-L., V. T. Moy, and H. E. Gaub. 1994. Adhesion force between individual ligand-receptor pairs. *Science.* 264:415–417.

Frishman, D., and P. Argos. 1995. Knowledge-based secondary structure assignment. *Proteins Struct. Funct. Genet.* 23:566–579.

Gat, Y., and M. Sheves. 1993. A mechanism for controlling the pK_a of the retinal protonated Schiff base in retinal proteins. A study with model compounds. *J. Am. Chem. Soc.* 115:3772–3773.

Greenhalgh, D. A., C. Altenbach, W. L. Hubbell, and H. G. Khorana. 1991. Locations of Arg-82, Asp-85, and Asp-96 in helix c of bacteriorhodopsin relative to the aqueous boundaries. *Proc. Natl. Acad. Sci. USA.* 88: 8626–8630.

Greenhalgh, D. A., D. L. Farrens, S. Subramaniam, and H. G. Khorana. 1993. Hydrophobic amino acids in the retinal-binding pocket of bacteriorhodopsin. *J. Biol. Chem.* 268:20305–20311.

Grigorieff, N., T. Ceska, K. Downing, J. Baldwin, and R. Henderson. 1996. Electron-crystallographic refinement of the structure of bacteriorhopsin. *J. Mol. Biol.* 259:393–421.

Grubmüller, H., B. Heymann, and P. Tavan. 1996. Ligand binding and molecular mechanics calculation of the streptavidin-biotin rupture force. *Science.* 271:997–999.

Hackett, N. R., L. J. Stern, B. H. Chao, K. A. Kronis, and H. G. Khorana. 1987. Structure-function studies on bacteriorhodopsin. V. Effects of amino acid substitutions in the putative helix f. *J. Biol. Chem.* 262: 9277–9284.

Henderson, R., J. M. Baldwin, T. A. Ceska, F. Zemlin, E. Beckmann, and K. H. Downing. 1990. Model for the structure of bacteriorhodopsin based on high-resolution electron cryo-microscopy. *J. Mol. Biol.* 213: 899–929.

Ho, M.-T. P., J. B. Massey, H. J. Pownall, R. E. Anderson, and J. G. Hollyfield. 1989. Mechanism of vitamin A movement between rod outer segments, interphotoreceptor retinoid-binding protein, and liposomes. *J. Biol. Chem.* 264:928–935.

Huang, K.-S., H. Bayley, M.-J. Liao, E. London, and H. G. Khorana. 1981. Refolding of an integral membrane protein. *J. Biol. Chem.* 256: 3802–3809.

Humphrey, W., I. Logunov, K. Schulten, and M. Sheves. 1994. Molecular dynamics study of bacteriorhodopsin and artificial pigments. *Biochemistry.* 33:3668–3678.

Humphrey, W., D. Xu, M. Sheves, and K. Schulten. 1995. Molecular dynamics study of the early intermediates in the bacteriorhodopsin photocycle. *J. Phys. Chem.* 99:14549–14560.

Izrailev, S., S. Stepaniants, M. Balsera, Y. Oono, and K. Schulten. 1997. Molecular dynamics study of unbinding of the avidin-biotin complex. *Biophys. J.* 72:1568–1581.

Khorana, H. G. 1988. Bacteriorhodopsin, a membrane protein that uses light to translocate protons. *J. Biol. Chem.* 263:7439–7442.

Khorana, H. G. 1993. Two light-transducing membrane proteins: Bacteriorhodopsin and the mammalian rhodopsin. *Proc. Natl. Acad. Sci. USA.* 90:1166–1171.

Krebs, M. P., and H. G. Khorana. 1993. Mechanism of light-dependent proton translocation by bacteriorhodopsin. *J. Bacteriol.* 175:1555–1560.

Lanyi, J. K. 1992. Proton-transfer and energy coupling in the bacteriorhodopsin photocycle. *J. Bioenerg. Biomembr.* 24:169–179.

London, E., and H. G. Khorana. 1982. Denaturation and renaturation of bacteriorhodopsin in detergents and lipid-detergent mixtures. *J. Biol. Chem.* 257:7003–7011.

Marti, T., H. Otto, T. Mogi, S. J. Rösselet, M. P. Heyn, and H. G. Khorana. 1991a. Bacteriorhodopsin mutants containing single substitutions of serine or threonine residues are all active in proton translocation. *J. Biol. Chem.* 266:6919–6927.

Marti, T., S. J. Rösselet, H. Otto, M. P. Heyn, and H. G. Khorana. 1991b. The retinylidene Schiff base counterion in bacteriorhodopsin. *J. Biol. Chem.* 266:18674–18683.

McCaslin, D. R., and C. Tanford. 1981. Effects of detergent micelles on the recombination reaction of opsin and 11-*cis*-retinal. *Biochemistry.* 20: 5207–5212.

Mierke, L. J. W., M. C. Betlach, A. K. Mitra, R. F. Shand, S. K. Fong, and R. M. Stroud. 1991. Wild-type and mutant bacteriorhodopsins D85N, D96N, and R82Q: purification to homogeneity, pH dependence of pumping, and electron diffraction. *Biochemistry.* 30:3088–3098.

Mogi, T., T. Marti, and H. G. Khorana. 1989a. Structure-function studies on bacteriorhodopsin. 9. Substitution of tryptophan residues affect protein-retinal interactions in bacteriorhodopsin. *J. Biol. Chem.* 264: 14197–14201.

Mogi, T., L. J. Stern, N. R. Hackett, and H. G. Khorana. 1987. Bacteriorhodopsin mutants containing single tyrosine to phenylalanine substitutions are all active in proton translocation. *Proc. Natl. Acad. Sci. USA.* 84:5595–5599.

Mogi, T., L. J. Stern, B. H. Chao, and H. G. Khorana. 1989b. Structure-function studies on bacteriorhodopsin. 8. Substitution of the membrane-embedded proline-50, proline-91, and proline-186—the effects are determined by the substituting amino acids. *J. Biol. Chem.* 264: 14192–14196.

Mogi, T., L. Stern, T. Marti, B. Chao, and H. Khorana. 1988. Aspartic acid substitutions affect proton translocation by bacteriorhodopsin. *Proc. Natl. Acad. Sci. USA.* 85:4148–4152.

Nonella, M., A. Windemuth, and K. Schulten. 1991. Structure of bacteriorhodopsin and in situ isomerization of retinal: a molecular dynamics study. *J. Photochem. Photobiol.* 54:937–948.

Oesterhelt, D., M. Meentzen, and L. Schumann. 1973. Reversible dissociation of the purple complex in bacteriorhodopsin and identification of 13-*cis* and all-*trans*-retinal as its chromophores. *Eur. J. Biochem.* 40: 453–463.

Oesterhelt, D., and L. Schumann. 1974. Reconstitution of bacteriorhodopsin. *FEBS Lett.* 44:262–265.

Oesterhelt, D., L. Schumann, and H. Gruber. 1974. Light-dependent reaction of bacteriorhodopsin with hydroxylamine in cell suspensions of *Halobacterium halobium*: demonstration of an apo-membrane. *FEBS Lett.* 44:257–261.

Oesterhelt, D., J. Tittor, and E. Bamberg. 1992. A unifying concept for ion translocation in retinal proteins. *J. Bioenerg. Biomembr.* 24:181–191.

Popot, J., and D. Engelman. 1990. Membrane protein folding and oligomerization: the two-stage model. *Biochemistry.* 29:4031.

Renthal, R., K. McMillan, L. Guerra, M. N. Garcia, R. Rangel, and C.-M. Jen. 1995. Long-range effects on the retinal chromophore of bacteriorhodopsin caused by surface carboxyl group modification. *Biochemistry.* 34:7869–7878.

Rousso, I., I. Brodsky, A. Lewis, and M. Sheves. 1995. The role of water in retinal complexation to bacterio-opsin. *J. Biol. Chem.* 270: 13860–13868.

Schulten, K., W. Humphrey, I. Logunov, M. Sheves, and D. Xu. 1995. Molecular dynamics studies of bacteriorhodopsin's photocycles. *Isr. J. Chem.* 35:447–464.

Stern, L. J., and H. G. Khorana. 1989. Structure-function studies on bacteriorhodopsin. Individual substitutions of arginine residues by glutamine affect chromophore formation, photocycle, and proton translocation. *J. Biol. Chem.* 264:14202–14208.

Subramaniam, S., D. A. Greenhalgh, P. Rath, K. J. Rotshild, and H. G. Khorana. 1991. Replacement of leucine-93 by alanine or threonine slows down the decay of the *n* and *o* intermediates in the photocycle of bacteriorhodopsin: implications for proton uptake and 13-*cis*-retinal → all-*trans*-retinal reisomerisation. *Proc. Natl. Acad. Sci. USA.* 88: 6873–6877.

Szuts, E. Z., and F. I. Harosi. 1991. Solubility of retinoids in water. *Arch. Biochem. Biophys.* 287:297–304.

Towner, P., W. Gaertner, B. Walckhoff, D. Osterhelt, and H. Hopf. 1981. Regeneration of rhodopsin and bacteriorhodopsin: the role of retinal analogues as inhibitors. *Eur. J. Biochem.* 117:353–359.

Unger, V. M., P. A. Hargrave, J. M. Baldwin, and F. X. Schertler. 1997. Arrangement of rhodopsin transmembrane α-helices. *Nature.* 389: 203–206.

Zingoni, J., Y. S. Or, R. K. Crouch, C.-H. Chang, R. Govindjee, and T. G. Ebrey. 1986. Effect of variation of retinal polyene side-chain length on formation and function of bacteriorhodopsin analogue pigments. *Biochemistry.* 25:2022–2027.